Optics Letters

Single-pixel imaging using compressed sensing and wavelength-dependent scattering

JAEWOOK SHIN, BRYAN T. BOSWORTH, AND MARK A. FOSTER*

Department of Electrical and Computer Engineering, Johns Hopkins University, Baltimore, Maryland 21218, USA
*Corresponding author: mark.foster@jhu.edu

Received 17 November 2015; revised 23 January 2016; accepted 23 January 2016; posted 25 January 2016 (Doc. ID 253900); published 18 February 2016

We demonstrate two-dimensional imaging using illumination via a single-mode fiber with a multiply scattering tip and compressed sensing acquisition. We illuminate objects with randomly structured, but deterministic, speckle patterns produced by a coherent light source propagating through a TiO_2-coated fiber tip. The coating thickness is optimized to produce speckle patterns that are highly sensitive to laser wavelength, yet repeatable. Images of the object are reconstructed from the characterized wavelength dependence of the speckle patterns and the wavelength dependence of the total light collected from the object using a single photodetector. Our imaging device is mechanically scan-free and insensitive to bending of the fiber, making it suitable for micro-endoscopy. © 2016 Optical Society of America

OCIS codes: (110.2350) Fiber optics imaging; (110.6150) Speckle imaging.

http://dx.doi.org/10.1364/OL.41.000886

Fiber endoscopes are extensively used to image the interior of the human or animal body. Recently, many investigations have been made in the field of micro-endoscopy to reduce the invasiveness of *in-vivo* imaging, while improving the image resolution and field of view (FOV). Conventional micro-endoscopes use a fiber bundle or multi-core fiber, where each fiber core transmits information from a single pixel of an object image. However, a fiber bundle can only contain several thousands of fiber cores, which limits the resolution of the output image and causes pixelation artifacts due to the spacing between the fiber cores. A typical fiber bundle endoscope has a diameter on the order of several millimeters, dictated by the core diameters, the total number of fiber cores in the bundle, and the core spacing needed to avoid cross-talk between cores. A notable alternative approach to designing an ultra-thin endoscope uses a single multi-mode fiber [1,2]. Such approach characterizes the multi-modal light propagation through the fiber, which is used in post-processing to reconstruct an object of interest. Unfortunately, the transmission matrix through a multi-mode fiber is extremely sensitive to bending of the fiber and requires active calibration and feedback to compensate for such fluctuations [3,4]. A second alternative approach is to use a one-dimensional spatial disperser at the end of a single-mode fiber to spectrally encode the object information [5]. While this approach measures spatial information in one transverse dimension without scanning, the image information in the other transverse dimension must still be acquired through scanning. In addition, a precise design of the distal end is required using a GRIN lens and a diffraction grating. In this Letter, we demonstrate a mechanically scan-free imaging approach using a single-mode fiber and a single photodetector through compressed sensing (CS) image reconstruction and the use of a multiply scattering medium.

In conventional imaging approaches, the raw data of an object image are acquired by serially scanning each pixel. The sampling device takes N measurements, where N is the total number of pixels in the object image. Using a sparsifying transform such as discrete wavelet or cosine transform, the raw image data is compressed by mapping to a sparse domain, and only the most significant coefficients are stored, while the rest of the data is thrown away [6]. Although the encoder can represent an object image using very few significant coefficients, a lot of the hardware resources used to sample the raw image are effectively wasted. Compressed sensing is a new sampling paradigm that implements such compression at the signal acquisition stage. Researchers in CS have proven that provided a signal is sparse in some basis, one can reconstruct the signal from far fewer measurements than the Nyquist sampling rate. Notably, in CS imaging pseudorandom patterns are extensively used to sample an object of interest, as they are strongly uncorrelated with the common mathematical bases in which natural images have sparse representations [7,8]. The inner products between these patterns and the object are the compressed measurements used to reconstruct the object by solving an optimization problem, such as minimizing the ℓ_1-norm of the object in its sparse form. Assuming the sampling patterns are sufficiently random to satisfy together the restricted isometry property (RIP), one can perfectly reconstruct the object image using M measurements, where $M \ll N$. For optical implementations of CS imaging, a digital micromirror device (DMD) is commonly employed to structure the incident wavefront and create pseudorandom illumination patterns or collection masks [9,10]. Such architectures are known as single-pixel imagers, since the inner product between the pseudorandom patterns and an object of interest are collected by a single photodetector instead of a CCD array.

Recently, image acquisition through a multiply scattering medium (zinc oxide) followed by spatially encoded measurements with a CCD was demonstrated as a simple and low-cost alternative to the conventional DMD approach [11]. Building on this demonstration, recent work demonstrates mapping of each wavelength of the illumination source to a 2D random spatial mask by characterizing the point spread function of each individual pixel of an object image received through a diffuser [12]. However, in this Letter, imaging performance was greatly hampered by the limited wavelength dependence of the light received through the scattering medium, which required a 6 nm wavelength step to produce a unique spatial structure and led to only 50 unique measurements over a 300 nm bandwidth spectrum collected off the object.

Here we show that by moving the scattering medium to the illumination side of the imager and optimizing the scattering medium thickness, unique spatial patterns are achieved with only 0.1 nm changes in the illumination wavelength and, therefore, 1000 unique measurements are acquired by scanning the laser illumination source by only 100 nm. Our imaging device consists of a near-infrared tunable continuous-wave laser source and a single-mode fiber with a titanium dioxide (TiO_2)-coated tip to generate two-dimensional (2D) illumination patterns of an object. The light from the object is collected with a lens and detected using a single photodector as a function of laser wavelength. We demonstrate that the optimized coating thickness of the scattering medium produces unique spatial patterns as the wavelength is tuned in 0.1 nm steps and that the patterns are repeatably realized in subsequent wavelength scans. Using compressed sensing algorithms, we reconstruct object images with far fewer measurements than those dictated by the Nyquist sampling theorem with high fidelity. Specifically, we reconstruct 218×218 pixel images of objects from 1000 measurements at different wavelengths using a total variation (TV) minimization algorithm.

A block diagram of the experimental system is shown in Fig. 1. The tunable continuous wave (CW) laser sweeps in wavelength from 1470 to 1569.9 nm in 0.1 nm increments to generate 1000 unique illumination patterns at the output of the 1.5 mm TiO_2-coated fiber tip. We experimentally determine that the TiO_2 coating has approximately 20% transmission of optical power. The light passes through a 20× objective lens to magnify the random illumination patterns at the object plane. The object plane is located one tube length away from the finite conjugate objective. A second focusing lens (FL) relays the infrared (IR) illumination patterns onto the IR camera for calibration. An iris (Ir) is employed to define the FOV and ensure that the IR camera and photodetector (PD) share the same FOV after the beam sampler (BS). Lastly, a 20× objective lens is used as a focusing lens to focus the light into the single PD. A neutral density filter (NDF) is used to attenuate the light incident on the IR camera. The IR camera, PD, and tunable laser are connected to a computer to automate data acquisition.

Two wavelength sweeps are performed to characterize the illumination patterns and then compressively acquire an image. The first sweep is performed for calibration of the imaging system, where random illumination patterns generated by the TiO_2-coated SMF are captured using the IR camera. At this

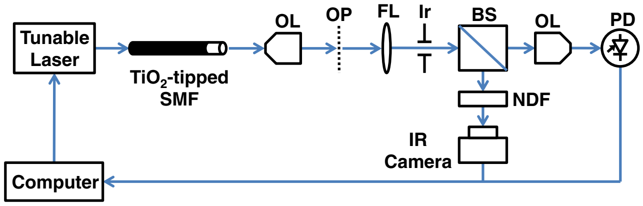

Fig. 1. Experimental setup of the compressive imaging device. TiO_2-tipped SMF = single-mode fiber coated with 1.5 mm of TiO_2; OL = 20× objective lens, OP = object plane; FL = focusing lens; Ir = iris; BS = beam sampler; PD = photodetector; NDF = neutral density filter.

stage, no object is placed at the object plane. The second sweep acquires the compressed measurements, where an object of interest (1951 USAF resolution target) is placed at the object plane. The random illumination patterns are projected onto the object, and their inner products are collected by the single PD.

One major principle of CS is that the sensing matrix must be highly uncorrelated within itself and with the sparsifying matrix to successfully reconstruct an object image. However, for this experimental system, there is an inherent trade-off between the randomness and repeatability of pattern generation, depending on the thickness of the scattering medium. Increasing the thickness of TiO_2 makes the illumination patterns more wavelength sensitive, ensuring that patterns from different wavelengths are maximally uncorrelated. However, if the illumination patterns are too wavelength sensitive, reliable calibration becomes difficult due to the limits on repeatability in the wavelength-stepped CW laser. Conversely, shortening the thickness of TiO_2 allows for repeatable wavelength-dependent scattering, but with reduced relative randomness of each illumination pattern, which reduces the total number of informative measurements possible given a limited wavelength scan range.

To optimize the pattern randomness and repeatability, the TiO_2 coating thickness is varied and the resulting illumination patterns for two independent wavelength sweeps are measured without any object placed in the object plane. The correlation between two random illumination patterns is calculated using

$$\mathrm{corr}(a, b) = \frac{\sum(a - \bar{a})(b - \bar{b})}{\sqrt{\sum(a - \bar{a})^2 \sum(b - \bar{b})^2}}, \qquad (1)$$

where a and b are random illumation patterns from the first and second sweep, while $\bar{a}$ and $\bar{b}$ are the means of the corresponding images. For a given thickness, a correlation is calculated for all pairs of illumination patterns in the wavelength sweep to generate the correlation plot in, for example, Fig. 2. The correlation among all of the wavelength-dependent patterns for these two sweeps is shown in Fig. 2 for a TiO_2 thickness of 1.5 mm. Note that the correlation between two independent random patterns should be as close to 0 (the correlation of a pattern with itself will be 1), demonstrating that this thickness strikes an appropriate balance between randomness and repeatability. As an example, Fig. 3 shows two pseudorandom illumination patterns at different wavelengths and their corresponding projections onto an object of interest.

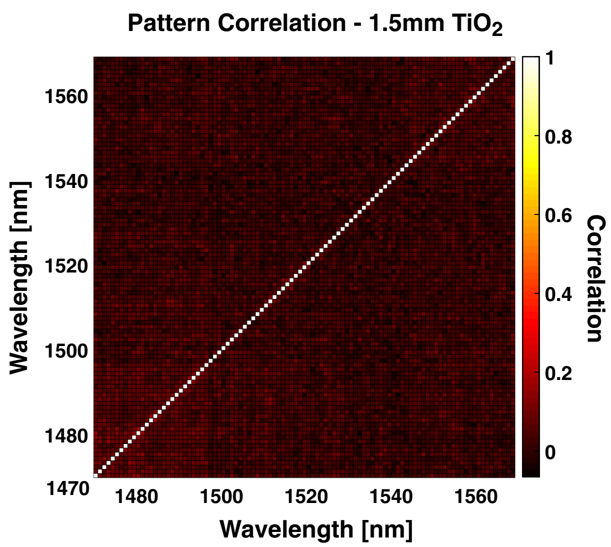

Fig. 2. Pattern correlation plot of the illumination patterns for 1.5 mm thickness of TiO_2.

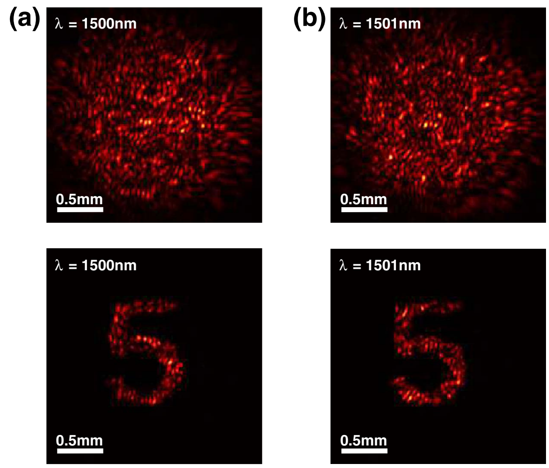

Fig. 3. (a) and (b) Random illumination patterns and their corresponding projections onto an object of interest at $\lambda = 1500$ nm and $\lambda = 1501$ nm.

Here, we assume that our object of interest is sparse in the spatial gradient domain. The spatial gradient of an image X of dimensions n_1 by n_2 is

$$g_{i,j} = \sqrt{(x_{i,j} - x_{i+1,j})^2 + (x_{i,j} - x_{i,j+1})^2}, \tag{2}$$

where $x_{i,j}$ is the $\{i, j\}$th pixel intensity of X. The total variation (TV) norm is defined as the summed magnitude of the spatial gradient:

$$\|x\|_{\mathrm{TV}} = \sum_{i=1}^{n_1} \sum_{j=1}^{n_2} g_{i,j}. \tag{3}$$

Let M and N represent the number of compressed measurements and the pixel dimensions of the object image ($N = n_1 \times n_2$), respectively. The observation vector $y \in \Re^{M\times 1}$ can be expressed as the following:

$$y = Ax = \begin{bmatrix} A_1 x \\ A_2 x \\ \vdots \\ A_M x \end{bmatrix}, \tag{4}$$

where $A_1, A_2, \ldots, A_M \in \Re^{1\times N}$ are the vectorized random illumination patterns, and $x \in \Re^{N\times 1}$ is the vectorized object image. The sensing matrix A consists of M random illumination patterns vertically concatenated, where $A \in \Re^{M\times N}$. We can recover the image of our object by solving the following optimization problem:

$$\underset{x}{\mathrm{argmin}} \|x\|_{\mathrm{TV}} \text{ s.t. } Ax = y, \qquad x \geq 0. \tag{5}$$

TV minimization by augmented Lagrangian and alternating direction algorithm (TVAL3) [13] is used to reconstruct the image. As shown in Eq. (2), the discrete gradient calculates the square root of summed squares of adjacent pixel intensity differences. Consequently, TV minimization algorithms are often used for edge detection, since it highlights regions of rapid intensity change.

Figure 4 shows successful reconstruction of 218 × 218 pixel images from 1000 different wavelength measurements in a single sweep, which corresponds to 2.1% compression or 47.5 × sub-Nyquist rate. The left-most column and middle column, respectively, consist of actual images of the objects taken with the IR camera and reconstructed images using the compressive measurements acquired with the photodetector. The right-most column shows the raw photodetector readings for the compressed measurements used in the TV minimization algorithm.

Although we assume sparsity in the spatial gradient to recover binary images in this Letter, the demonstrated imaging device is suitable for imaging generalized objects in, for example, an endoscopy application. The strength of pseudorandom sampling in CS imaging is that one can recover an object image, as long as it can be sparsely represented in some known basis. Real images are known to be highly compressible via image encoding techniques such as the JPEG or JPEG2000 standards, which use DCT and wavelet bases, respectively. In other words, countless types of objects can be accurately imaged using the exact same set of physical measurements simply by employing a different sparsifying basis in the reconstruction algorithm.

Additionally, objects of interest embedded in a scattering volume can generate unwanted changes to the speckle pattern that can degrade the performance of this system. This perturbation can be modeled for the reconstruction as additional noise n, varying by wavelength, added to the measurement patterns: $A' = A + n$. CS theory states that signal reconstruction will be successful provided the observations contaminated by noise, i.e., $y = A'x = Ax + w$, are bounded by a known amount $\|w\|_2 \leq \sigma$ [7,8]. One can recover x from noisy measurements by solving the following optimization problem:

$$\underset{x}{\mathrm{argmin}} \|x\|_{\mathrm{TV}} \text{ s.t. } \|y - Ax\|_2 \leq \sigma, \qquad x \geq 0. \tag{6}$$

In other words, one can successfully reconstruct object images provided the perturbations are small, while significant changes to the calibrated speckle patterns can degrade the reconstruction.

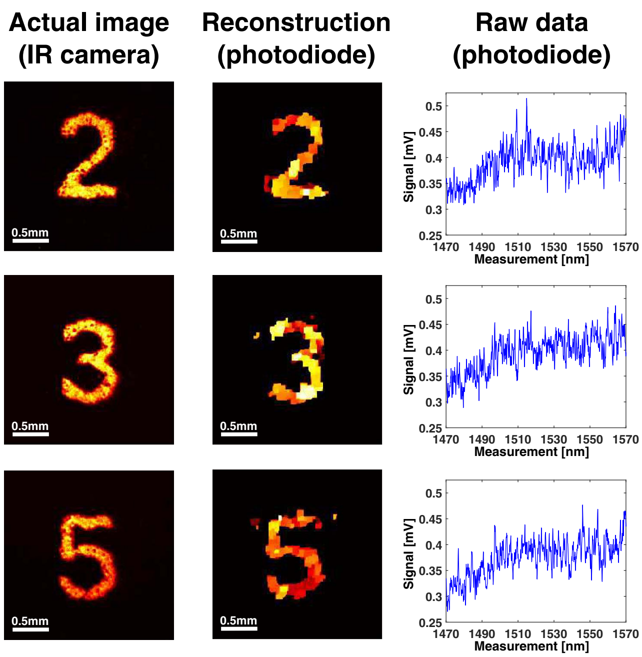

Fig. 4. Reconstruction of digits from 1951 USAF resolution target. Actual images of the objects taken with a IR camera are shown in the left-most column; reconstruction results are shown in the middle column; raw photodiode measurements are plotted in the right-most column. Scale bar = 0.5 mm.

In conclusion, we have designed a single-pixel compressive imager using a single-mode fiber coated with a wavelength-sensitive scattering medium. Our imaging technique is mechanically scan-free and insensitive to bending of the fiber, an advantage for micro-endoscopy applications, as well as wavelength-encoded high-throughput imaging [14,15]. In addition, our structured illumination approach can be readily realized in the visible spectrum for fluorescence imaging. Toward endoscopy, one future approach is to use a dual-core fiber, where a small single-mode core is used for illumination, and the light from the object is collected back through the fiber using a much larger multi-mode core. Additionally, beyond CS, multiply scattering media hold great potential as a superlens to exceed the diffraction limit of a conventional lens [16,17]. While the numerical aperture of a conventional lens is limited by its most oblique angle and, thus, its physical dimensions, scattering media allow for the collection of a wider range of spatial frequencies of incoming light due to the scattering process and thus higher spatial resolution and FOV. We expect that these additional benefits can also be leveraged in future realizations of our approach.

Funding. National Science Foundation (NSF) (ECCS-1254610).

REFERENCES

1. R. N. Mahalati, R. Y. Gu, and J. M. Kahn, Opt. Express **21**, 1656 (2013).
2. Y. Choi, C. Yoon, M. Kim, T. D. Yang, C. Fang-Yen, R. R. Dasari, K. J. Lee, and W. Choi, Phys. Rev. Lett. **109**, 203901 (2012).
3. A. Caravaca-Aguirre, E. Niv, D. Conkey, and R. Piestun, Opt. Express **21**, 12881 (2013).
4. S. Farahi, D. Ziegler, I. Papadopoulos, D. Psaltis, and C. Moser, Opt. Express **21**, 22504 (2013).
5. D. Yelin, W. M. White, J. T. Motz, S. H. Yun, B. E. Bouma, and G. J. Tearney, Opt. Express **15**, 2432 (2007).
6. S. Mallat, *A Wavelet Tour of Signal Processing: The Sparse Way* (Academic, 2008).
7. E. J. Candes, J. K. Romberg, and T. Tao, Commun. Pure Appl. Math. **59**, 1207 (2006).
8. E. J. Candès and M. B. Wakin, IEEE Signal Process. Mag. **25**, 21 (2008).
9. M. F. Duarte, M. A. Davenport, D. Takhar, J. N. Laska, T. Sun, K. F. Kelly, and R. G. Baraniuk, IEEE Signal Process. Mag. **25**, 83 (2008).
10. V. Studer, J. Bobin, M. Chahid, H. S. Mousavi, E. Candes, and M. Dahan, Proc. Natl. Acad. Sci. USA **109**, E1679 (2012).
11. A. Liutkus, D. Martina, S. Popoff, G. Chardon, O. Katz, G. Lerosey, S. Gigan, L. Daudet, and I. Carron, Sci. Rep. **4**, 5552 (2014).
12. S. M. Kolenderska, O. Katz, M. Fink, and S. Gigan, Opt. Lett. **40**, 534 (2015).
13. C. Li, W. Yin, H. Jiang, and Y. Zhang, Comput. Optim. Appl. **56**, 507 (2013).
14. K. Goda, K. Tsia, and B. Jalali, Nature **458**, 1145 (2009).
15. B. Bosworth, J. Stroud, D. Tran, T. Tran, S. Chin, and M. Foster, Opt. Express **23**, 10521 (2015).
16. Y. Choi, T. Yang, C. Yen, P. Kang, K. Lee, R. Dasari, M. Feld, and W. Choi, Phys. Rev. Lett. **107**, 023902 (2011).
17. I. M. Vellekoop, A. Lagendijk, and A. P. Mosk, Nat. Photonics **4**, 320 (2010).